



Improved measurement of $B^0 \rightarrow \pi^0 \pi^0$

K. Abe,⁹ K. Abe,⁴⁹ I. Adachi,⁹ H. Aihara,⁵¹ D. Anipko,¹ K. Aoki,²⁵ T. Arakawa,³²
 K. Arinstein,¹ Y. Asano,⁵⁶ T. Aso,⁵⁵ V. Aulchenko,¹ T. Aushev,²¹ T. Aziz,⁴⁷ S. Bahinipati,⁴
 A. M. Bakich,⁴⁶ V. Balagura,¹⁵ Y. Ban,³⁷ S. Banerjee,⁴⁷ E. Barberio,²⁴ M. Barbero,⁸
 A. Bay,²¹ I. Bedny,¹ K. Belous,¹⁴ U. Bitenc,¹⁶ I. Bizjak,¹⁶ S. Blyth,²⁷ A. Bondar,¹
 A. Bozek,³⁰ M. Bračko,^{23,16} J. Brodzicka,^{9,30} T. E. Browder,⁸ M.-C. Chang,⁵⁰ P. Chang,²⁹
 Y. Chao,²⁹ A. Chen,²⁷ K.-F. Chen,²⁹ W. T. Chen,²⁷ B. G. Cheon,³ R. Chistov,¹⁵
 J. H. Choi,¹⁸ S.-K. Choi,⁷ Y. Choi,⁴⁵ Y. K. Choi,⁴⁵ A. Chuvikov,³⁹ S. Cole,⁴⁶ J. Dalseno,²⁴
 M. Danilov,¹⁵ M. Dash,⁵⁷ R. Dowd,²⁴ J. Dragic,⁹ A. Drutskoy,⁴ S. Eidelman,¹ Y. Enari,²⁵
 D. Epifanov,¹ S. Fratina,¹⁶ H. Fujii,⁹ M. Fujikawa,²⁶ N. Gabyshev,¹ A. Garmash,³⁹
 T. Gershon,⁹ A. Go,²⁷ G. Gokhroo,⁴⁷ P. Goldenzweig,⁴ B. Golob,^{22,16} A. Gorišek,¹⁶
 M. Grosse Perdekamp,^{11,40} H. Guler,⁸ H. Ha,¹⁸ J. Haba,⁹ K. Hara,²⁵ T. Hara,³⁵
 Y. Hasegawa,⁴⁴ N. C. Hastings,⁵¹ K. Hayasaka,²⁵ H. Hayashii,²⁶ M. Hazumi,⁹
 D. Heffernan,³⁵ T. Higuchi,⁹ L. Hinz,²¹ T. Hokuue,²⁵ Y. Hoshi,⁴⁹ K. Hoshina,⁵⁴ S. Hou,²⁷
 W.-S. Hou,²⁹ Y. B. Hsiung,²⁹ Y. Igarashi,⁹ T. Iijima,²⁵ K. Ikado,²⁵ A. Imoto,²⁶ K. Inami,²⁵
 A. Ishikawa,⁵¹ H. Ishino,⁵² K. Itoh,⁵¹ R. Itoh,⁹ M. Iwabuchi,⁶ M. Iwasaki,⁵¹ Y. Iwasaki,⁹
 C. Jacoby,²¹ M. Jones,⁸ H. Kakuno,⁵¹ J. H. Kang,⁵⁸ J. S. Kang,¹⁸ P. Kapusta,³⁰
 S. U. Kataoka,²⁶ N. Katayama,⁹ H. Kawai,² T. Kawasaki,³² H. R. Khan,⁵² A. Kibayashi,⁵²
 H. Kichimi,⁹ N. Kikuchi,⁵⁰ H. J. Kim,²⁰ H. O. Kim,⁴⁵ J. H. Kim,⁴⁵ S. K. Kim,⁴³
 T. H. Kim,⁵⁸ Y. J. Kim,⁶ K. Kinoshita,⁴ N. Kishimoto,²⁵ S. Korpar,^{23,16} Y. Kozakai,²⁵
 P. Križan,^{22,16} P. Krokovny,⁹ T. Kubota,²⁵ R. Kulasiri,⁴ R. Kumar,³⁶ C. C. Kuo,²⁷
 E. Kurihara,² A. Kusaka,⁵¹ A. Kuzmin,¹ Y.-J. Kwon,⁵⁸ J. S. Lange,⁵ G. Leder,¹³ J. Lee,⁴³
 S. E. Lee,⁴³ Y.-J. Lee,²⁹ T. Lesiak,³⁰ J. Li,⁸ A. Limosani,⁹ C. Y. Lin,²⁹ S.-W. Lin,²⁹
 Y. Liu,⁶ D. Liventsev,¹⁵ J. MacNaughton,¹³ G. Majumder,⁴⁷ F. Mandl,¹³ D. Marlow,³⁹
 T. Matsumoto,⁵³ A. Matyja,³⁰ S. McOnie,⁴⁶ T. Medvedeva,¹⁵ Y. Mikami,⁵⁰ W. Mitaroff,¹³
 K. Miyabayashi,²⁶ H. Miyake,³⁵ H. Miyata,³² Y. Miyazaki,²⁵ R. Mizuk,¹⁵ D. Mohapatra,⁵⁷
 G. R. Moloney,²⁴ T. Mori,⁵² J. Mueller,³⁸ A. Murakami,⁴¹ T. Nagamine,⁵⁰ Y. Nagasaka,¹⁰
 T. Nakagawa,⁵³ Y. Nakahama,⁵¹ I. Nakamura,⁹ E. Nakano,³⁴ M. Nakao,⁹ H. Nakazawa,⁹
 Z. Natkaniec,³⁰ K. Neichi,⁴⁹ S. Nishida,⁹ K. Nishimura,⁸ O. Nitoh,⁵⁴ S. Noguchi,²⁶
 T. Nozaki,⁹ A. Ogawa,⁴⁰ S. Ogawa,⁴⁸ T. Ohshima,²⁵ T. Okabe,²⁵ S. Okuno,¹⁷ S. L. Olsen,⁸
 S. Ono,⁵² W. Ostrowicz,³⁰ H. Ozaki,⁹ P. Pakhlov,¹⁵ G. Pakhlova,¹⁵ H. Palka,³⁰
 C. W. Park,⁴⁵ H. Park,²⁰ K. S. Park,⁴⁵ N. Parslow,⁴⁶ L. S. Peak,⁴⁶ M. Pernicka,¹³
 R. Pestotnik,¹⁶ M. Peters,⁸ L. E. Piilonen,⁵⁷ A. Poluektov,¹ F. J. Ronga,⁹ N. Root,¹
 J. Rorie,⁸ M. Rozanska,³⁰ H. Sahoo,⁸ S. Saitoh,⁹ Y. Sakai,⁹ H. Sakamoto,¹⁹ H. Sakaue,³⁴
 T. R. Sarangi,⁶ N. Sato,²⁵ N. Satoyama,⁴⁴ K. Sayeed,⁴ T. Schietinger,²¹ O. Schneider,²¹
 P. Schönmeier,⁵⁰ J. Schümann,²⁸ C. Schwanda,¹³ A. J. Schwartz,⁴ R. Seidl,^{11,40} T. Seki,⁵³
 K. Senyo,²⁵ M. E. Sevior,²⁴ M. Shapkin,¹⁴ Y.-T. Shen,²⁹ H. Shibuya,⁴⁸ B. Shwartz,¹

V. Sidorov,¹ J. B. Singh,³⁶ A. Sokolov,¹⁴ A. Somov,⁴ N. Soni,³⁶ R. Stamen,⁹ S. Stanič,³³
M. Starič,¹⁶ H. Stoeck,⁴⁶ A. Sugiyama,⁴¹ K. Sumisawa,⁹ T. Sumiyoshi,⁵³ S. Suzuki,⁴¹
S. Y. Suzuki,⁹ O. Tajima,⁹ N. Takada,⁴⁴ F. Takasaki,⁹ K. Tamai,⁹ N. Tamura,³²
K. Tanabe,⁵¹ M. Tanaka,⁹ G. N. Taylor,²⁴ Y. Teramoto,³⁴ X. C. Tian,³⁷ I. Tikhomirov,¹⁵
K. Trabelsi,⁹ Y. T. Tsai,²⁹ Y. F. Tse,²⁴ T. Tsuboyama,⁹ T. Tsukamoto,⁹ K. Uchida,⁸
Y. Uchida,⁶ S. Uehara,⁹ T. Uglov,¹⁵ K. Ueno,²⁹ Y. Unno,⁹ S. Uno,⁹ P. Urquijo,²⁴
Y. Ushiroda,⁹ Y. Usov,¹ G. Varner,⁸ K. E. Varvell,⁴⁶ S. Villa,²¹ C. C. Wang,²⁹
C. H. Wang,²⁸ M.-Z. Wang,²⁹ M. Watanabe,³² Y. Watanabe,⁵² J. Wicht,²¹ L. Widhalm,¹³
J. Wiechczynski,³⁰ E. Won,¹⁸ C.-H. Wu,²⁹ Q. L. Xie,¹² B. D. Yabsley,⁴⁶ A. Yamaguchi,⁵⁰
H. Yamamoto,⁵⁰ S. Yamamoto,⁵³ Y. Yamashita,³¹ M. Yamauchi,⁹ Heyoung Yang,⁴³
S. Yoshino,²⁵ Y. Yuan,¹² Y. Yusa,⁵⁷ S. L. Zang,¹² C. C. Zhang,¹² J. Zhang,⁹
L. M. Zhang,⁴² Z. P. Zhang,⁴² V. Zhilich,¹ T. Ziegler,³⁹ A. Zupanc,¹⁶ and D. Zürcher²¹

(The Belle Collaboration)

¹*Budker Institute of Nuclear Physics, Novosibirsk*

²*Chiba University, Chiba*

³*Chonnam National University, Kwangju*

⁴*University of Cincinnati, Cincinnati, Ohio 45221*

⁵*University of Frankfurt, Frankfurt*

⁶*The Graduate University for Advanced Studies, Hayama*

⁷*Gyeongsang National University, Chinju*

⁸*University of Hawaii, Honolulu, Hawaii 96822*

⁹*High Energy Accelerator Research Organization (KEK), Tsukuba*

¹⁰*Hiroshima Institute of Technology, Hiroshima*

¹¹*University of Illinois at Urbana-Champaign, Urbana, Illinois 61801*

¹²*Institute of High Energy Physics,*

Chinese Academy of Sciences, Beijing

¹³*Institute of High Energy Physics, Vienna*

¹⁴*Institute of High Energy Physics, Protvino*

¹⁵*Institute for Theoretical and Experimental Physics, Moscow*

¹⁶*J. Stefan Institute, Ljubljana*

¹⁷*Kanagawa University, Yokohama*

¹⁸*Korea University, Seoul*

¹⁹*Kyoto University, Kyoto*

²⁰*Kyungpook National University, Taegu*

²¹*Swiss Federal Institute of Technology of Lausanne, EPFL, Lausanne*

²²*University of Ljubljana, Ljubljana*

²³*University of Maribor, Maribor*

²⁴*University of Melbourne, Victoria*

²⁵*Nagoya University, Nagoya*

²⁶*Nara Women's University, Nara*

²⁷*National Central University, Chung-li*

²⁸*National United University, Miao Li*

²⁹*Department of Physics, National Taiwan University, Taipei*

³⁰*H. Niewodniczanski Institute of Nuclear Physics, Krakow*

³¹*Nippon Dental University, Niigata*

³²*Niigata University, Niigata*
³³*University of Nova Gorica, Nova Gorica*
³⁴*Osaka City University, Osaka*
³⁵*Osaka University, Osaka*
³⁶*Panjab University, Chandigarh*
³⁷*Peking University, Beijing*
³⁸*University of Pittsburgh, Pittsburgh, Pennsylvania 15260*
³⁹*Princeton University, Princeton, New Jersey 08544*
⁴⁰*RIKEN BNL Research Center, Upton, New York 11973*
⁴¹*Saga University, Saga*
⁴²*University of Science and Technology of China, Hefei*
⁴³*Seoul National University, Seoul*
⁴⁴*Shinshu University, Nagano*
⁴⁵*Sungkyunkwan University, Suwon*
⁴⁶*University of Sydney, Sydney NSW*
⁴⁷*Tata Institute of Fundamental Research, Bombay*
⁴⁸*Toho University, Funabashi*
⁴⁹*Tohoku Gakuin University, Tagajo*
⁵⁰*Tohoku University, Sendai*
⁵¹*Department of Physics, University of Tokyo, Tokyo*
⁵²*Tokyo Institute of Technology, Tokyo*
⁵³*Tokyo Metropolitan University, Tokyo*
⁵⁴*Tokyo University of Agriculture and Technology, Tokyo*
⁵⁵*Toyama National College of Maritime Technology, Toyama*
⁵⁶*University of Tsukuba, Tsukuba*
⁵⁷*Virginia Polytechnic Institute and State University, Blacksburg, Virginia 24061*
⁵⁸*Yonsei University, Seoul*

Abstract

We report an improved measurement of the decay $B^0 \rightarrow \pi^0\pi^0$, using a data sample of $535 \times 10^6 B\bar{B}$ pairs collected at the $\Upsilon(4S)$ resonance with the Belle detector at the KEKB asymmetric-energy e^+e^- collider. The measured branching fraction is $\mathcal{B}(B^0 \rightarrow \pi^0\pi^0) = (1.1 \pm 0.3(\text{stat.}) \pm 0.1(\text{syst.})) \times 10^{-6}$, with a significance of 5.4 standard deviations including systematic uncertainties. We also report the partial rate asymmetry: $\mathcal{A}_{CP}(B^0 \rightarrow \pi^0\pi^0) = 0.44^{+0.73}_{-0.62}(\text{stat.})^{+0.04}_{-0.06}(\text{syst.})$.

PACS numbers: 11.30.Er, 12.15.Hh, 13.25.Hw, 14.40.Nd

Measurements of the mixing-induced CP violation parameter $\sin 2\phi_1$ [1, 2] at B factories are in good agreement with the Kobayashi-Maskawa (KM) mechanism [3]. To confirm this theory, one now has to measure the other two angles of the unitarity triangle, ϕ_2 and ϕ_3 . One technique for measuring ϕ_2 is to study time-dependent CP asymmetries in $B^0 \rightarrow \pi^+\pi^-$ decay, where both Belle [4] and BaBar [5] recently reported the observation of mixing-induced CP violation. Belle observed direct CP violation while BaBar found no direct CP violation. The extraction of ϕ_2 , however, is complicated by the presence of both tree and penguin amplitudes, each with different weak phases. An isospin analysis of the $\pi\pi$ system is necessary [6], and one essential ingredient is the branching fraction for the decay $B^0 \rightarrow \pi^0\pi^0$.

QCD-based factorization predictions for $\mathcal{B}(B^0 \rightarrow \pi^0\pi^0)$ are typically around or below 1×10^{-6} [7], but phenomenological models incorporating large rescattering effects can accommodate larger values [8]. Observation for $B^0 \rightarrow \pi^0\pi^0$ was previously reported by Belle with the value of $(2.3^{+0.4}_{-0.5}(\text{stat.})^{+0.2}_{-0.3}(\text{syst.})) \times 10^{-6}$ for the branching fraction [9]. If such a high value persists, an isospin analysis for ϕ_2 extraction would become feasible in the near future. To complete the program, one would need to measure both the B^0 and \bar{B}^0 decay rates, i.e. direct CP violation.

In this paper we report the improved measurement of the decay $B^0 \rightarrow \pi^0\pi^0$. We also provide a measurement of the direct CP violating asymmetry in this mode. The results are based on a $535 \times 10^6 B\bar{B}$ pairs, collected with the Belle detector at the KEKB asymmetric-energy e^+e^- (3.5 on 8 GeV) collider [10].

The Belle detector is a large-solid-angle magnetic spectrometer that consists of a silicon vertex detector (SVD), a 50-layer central drift chamber (CDC), an array of aerogel threshold Čerenkov counters (ACC), a barrel-like arrangement of time-of-flight scintillation counters (TOF), and an electromagnetic calorimeter comprised of CsI(Tl) crystals (ECL) located inside a super-conducting solenoid coil that provides a 1.5 T magnetic field. An iron flux-return located outside of the coil is instrumented to detect K_L^0 mesons and to identify muons (KLM). The detector is described in detail elsewhere [11]. Two inner detector configurations were used. A 2.0 cm beampipe and a 3-layer silicon vertex detector were used for the first sample of $152 \times 10^6 B\bar{B}$ pairs (Set I), while a 1.5 cm beampipe, a 4-layer silicon detector and a small-cell inner drift chamber [12] were used to record the remaining $383 \times 10^6 B\bar{B}$ pairs (Set II).

Pairs of photons with invariant masses in the range $115 \text{ MeV}/c^2 < m_{\gamma\gamma} < 152 \text{ MeV}/c^2$ are used to form π^0 mesons and π^0 mass constraint is implemented; this corresponds to a window of $\pm 2.5\sigma$ about the nominal π^0 mass, where σ denotes the experimental resolution, approximately $8 \text{ MeV}/c^2$. The measured energy of each photon in the laboratory frame is required to be greater than 50 MeV in the barrel region, defined as $32^\circ < \theta_\gamma < 129^\circ$, and greater than 100 MeV in the end-cap regions, defined as $17^\circ \leq \theta_\gamma \leq 32^\circ$ and $129^\circ \leq \theta_\gamma \leq 150^\circ$, where θ_γ denotes the polar angle of the photon with respect to the positron beam line. To further reduce the combinatorial background, π^0 candidates with small decay angles ($\cos \theta^* > 0.95$) are rejected, where θ^* is the angle between the π^0 boost direction from the laboratory frame and one of its γ daughters in the π^0 rest frame.

Signal B candidates are formed from pairs of π^0 mesons and are identified by their beam energy constrained mass $M_{bc} = \sqrt{E_{\text{beam}}^{*2}/c^4 - p_B^{*2}/c^2}$ and energy difference $\Delta E = E_B^* - E_{\text{beam}}^*$, where E_{beam}^* denotes the run-dependent beam energy, p_B^* and E_B^* are the reconstructed momentum and energy of the B candidates, all in the e^+e^- CM frame. We require $M_{bc} > 5.2 \text{ GeV}/c^2$ and $-0.45 \text{ GeV} < \Delta E < 0.5 \text{ GeV}$. The signal efficiency is estimated using GEANT-based [13] Monte Carlo (MC) simulations. The resolution for

signal is approximately $3.6 \text{ MeV}/c^2$ in M_{bc} . The distribution in ΔE is asymmetric due to energy leakage from the CsI(Tl) crystals.

We consider background from other B decays and from $e^+e^- \rightarrow q\bar{q}$ ($q = u, d, s, c$) continuum processes. A large generic MC sample shows that backgrounds from $b \rightarrow c$ decays are negligible. Among charmless B decays, the only significant background is $B^\pm \rightarrow \rho^\pm \pi^0$ with a missing low momentum π^\pm . This background populates the negative ΔE region, and is taken into account in the signal extraction described below.

The dominant background is due to the continuum processes. We use event topology to discriminate signal events from this $q\bar{q}$ background, and follow the continuum rejection technique from our previous publication [9]. We combine a set of modified Fox-Wolfram moments [14] into a Fisher discriminant [15]. A signal/background likelihood is formed, based on a Monte Carlo (MC) simulation for signal and events in the M_{bc} sideband region ($5.20 \text{ GeV}/c^2 < M_{bc} < 5.26 \text{ GeV}/c^2$) for the $q\bar{q}$ background, from the product of the probability density functions (PDFs) for the Fisher discriminant and that for the cosine of the angle between the B -meson flight direction and the positron beam. The continuum suppression is achieved by applying a requirement on a likelihood ratio $\mathcal{R}_{\text{sig}} = \mathcal{L}_{\text{sig}} / (\mathcal{L}_{\text{sig}} + \mathcal{L}_{q\bar{q}})$, where \mathcal{L}_{sig} ($\mathcal{L}_{q\bar{q}}$) is the signal ($q\bar{q}$) likelihood.

Additional discrimination between signal and background can be achieved by using the Belle standard algorithm for b -flavor tagging [16], which is also needed for the direct CP violation measurement. The flavor tagging procedure yields two outputs: $q = \pm 1$, indicating the flavor of the other B in the event, and r , which takes values between 0 and 1 and is a measure of the confidence that the q determination is correct. Events with a high value of r are considered well-tagged and are therefore unlikely to have originated from continuum processes. For example, an event that contains a high momentum lepton (r close to unity) is more likely to be a $B\bar{B}$ event so a looser \mathcal{R}_{sig} requirement can be applied. We find that there is no strong correlation between r and any of the topological variables used above to separate signal from the continuum.

We divide the data into $r \geq 0.5$ and $r < 0.5$ bins. The continuum background is reduced by applying a selection requirement on \mathcal{R}_{sig} for events in each r region of Set I and Set II according to the figure of merit (FOM). The FOM is defined as $N_{\text{sig}}^{\text{exp}} / \sqrt{N_{\text{sig}}^{\text{exp}} + N_{\text{bg}}^{\text{exp}}}$, where $N_{\text{sig}}^{\text{exp}}$ and $N_{\text{bg}}^{\text{exp}}$ denote the expected signal, assuming the branching fraction $\mathcal{B} = 2 \times 10^{-6}$, and background yields obtained from $B^\pm \rightarrow \rho^\pm \pi^0$ MC and sideband data, respectively. A typical requirement suppresses 98% of the continuum background while retaining 45% of the signal.

In our previous publications [9, 17] we reported a special background originating from the overlap of a hadronic continuum event and the residual calorimeter energies from an earlier QED scattering event. This $e^+e^- \rightarrow \gamma\gamma$ background has a signature of back-to-back photons in the CM frame, which can combine with two soft photons to form $\pi^0\pi^0$ candidates. The fake $\pi^0\pi^0$ candidates tend to have very small total CM momenta due to the characteristics of the back-to-back photons, resulting in a peaking behavior at $M_{bc} = 5.28 \text{ GeV}/c^2$. Therefore the QED background is quite similar to the $B^0 \rightarrow \pi^0\pi^0$ signal and has to be considered in the signal extraction. The best way to identify the $e^+e^- \rightarrow \gamma\gamma$ events is to use the timing information of the ECL clusters, which are off-time for the QED background but only available in the latter 239 fb^{-1} of data. For data in which the timing information is not available, we have to rely on other observables to distinguish candidates synchronized with the trigger particles (on-time) from the off-time QED background. Assuming the distributions of the off-time QED background are the same for the first 253 fb^{-1} and latter

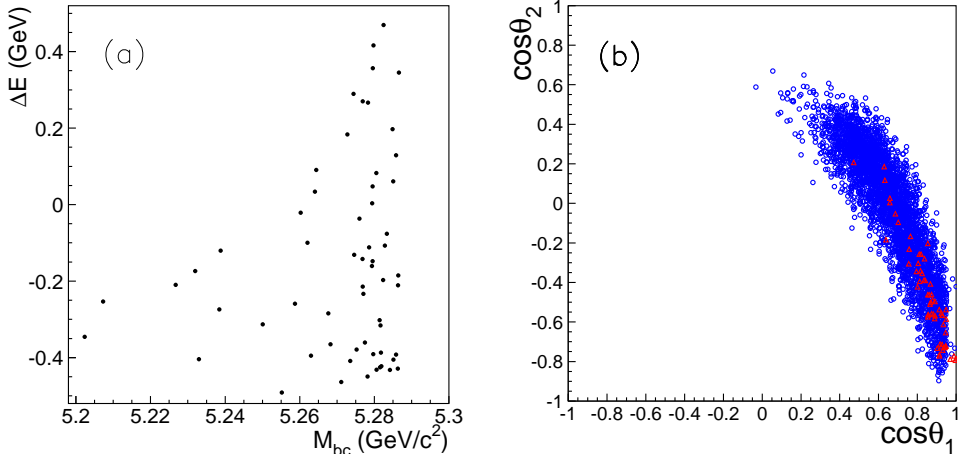


FIG. 1: (a) The distribution of ΔE vs. M_{bc} for the off-time events; (b) the distributions of $\cos \theta_2$ vs. $\cos \theta_1$ for the on-time events (circle) and the off-time events (triangle).

239 fb^{-1} , the PDFs of the observables can be obtained using the data in the latter 239 fb^{-1} sample, in which trigger timing information can be used to identify the on-time and off-time events.

Figure 1(a) shows the M_{bc} - ΔE distribution for the off-time $\pi^0\pi^0$ candidates in the latter 239 fb^{-1} sample after passing all analysis requirements. These off-time $\pi^0\pi^0$ events are located in the M_{bc} signal region but have no particular structure in ΔE . Since the QED photons are close to the e^+ and e^- directions, the angle between the π^0 moving direction and the z axis can be used to identify the QED background. The angular distributions of on-time and off-time candidates in the latter sample are shown in Fig. 1(b), where θ_1 and θ_2 are the angles of higher and lower momentum π^0 s, respectively. Compared to the on-time events, the off-time candidates have a narrow distribution in $(\cos \theta_1, \cos \theta_2)$ -plane. The last variable that helps distinguish the QED background is missing energy, defined as $E_{\text{miss}} = E_{\text{total}}^* - 2 E_{\text{beam}}^*$, where E_{total}^* is the total reconstructed energy in the CM frame. Since the QED background consists of two overlapping events, the missing energy tends to be larger than that of the on-time events. All these five observables are implemented in the fit.

The signal yields are extracted by applying unbinned five-dimensional maximum likelihood (ML) fits to the $(M_{bc}, \Delta E, \cos \theta_1, \cos \theta_2, E_{\text{miss}})$ distributions of the B and \overline{B} samples. The likelihood is defined as

$$\mathcal{L} = \exp \left(- \sum_{s,k,j} N_{s,k,j} \right) \prod_i \left(\sum_{s,k,j} N_{s,k,j} \mathcal{P}_{s,k,j}^i \right) \quad (1)$$

where

$$\mathcal{P}_{s,k,j}^i = \frac{1}{2} [1 - q^i \cdot \mathcal{A}_{CP}] P1_{s,k,j}(M_{bc}^i, \Delta E^i) \times P2_{s,k,j}(\cos \theta_1^i, \cos \theta_2^i) \times P3_{s,k,j}(E_{\text{miss}}^i). \quad (2)$$

The direct CP asymmetry is defined as

$$\mathcal{A}_{CP} \equiv \frac{N(\overline{B} \rightarrow \overline{f}) - N(B \rightarrow f)}{N(\overline{B} \rightarrow \overline{f}) + N(B \rightarrow f)}, \quad (3)$$

and s indicates Set I or Set II, k distinguishes events in the $r < 0.5$ or $r \geq 0.5$ bins, j indicates the category of signal or background contributions due to the $q\bar{q}$ continuum, $B^\pm \rightarrow \rho^\pm \pi^0$ decay and off-time QED events. i is the identifier of the i -th event, $P1_{s,k,j}(M_{bc}, \Delta E)$ are the two-dimensional probability density functions (PDFs) in M_{bc} and ΔE , $P2_{s,k,j}(\cos \theta_1, \cos \theta_2)$ are the two-dimensional PDFs in $\cos \theta_1$ and $\cos \theta_2$, $P3_{s,k,j}(E_{\text{miss}})$ are the one-dimensional PDFs in E_{miss} , $N_{s,k,j}$ is the number of events and q^i indicates the B meson flavor: $q^i = +1(-1)$ for B^0 and \overline{B}^0 . The flavor of the B meson in the $B^0 \rightarrow \pi^0 \pi^0$ channel is not self-tagged and must be determined from the accompanying B meson. To account for the effect of B^0 - \overline{B}^0 mixing and imperfect tagging, the term \mathcal{A}_{CP} for the signal in Eq. 2 has to be replaced by $\mathcal{A}_{CP}(1 - 2\chi_d)(1 - 2w_k)$, where $\chi_d = 0.186 \pm 0.004$ [18] is the time-integrated mixing parameter and w_k is the wrong-tag fraction that depends on the value of r . The wrong-tag fractions are determined using a large sample of self-tagged $B^0 \rightarrow D^{*-} \pi^+$, $D^{*-} \rho^+$ and $D^{(*)-} l^+ \nu$ events and their charge conjugates [16].

The M_{bc} - ΔE PDFs for the signal and for the $B^+ \rightarrow \rho^+ \pi^0$ background are taken from smoothed two-dimensional histograms obtained from large MC samples. For the signal PDF ($P1$), discrepancies between the peak positions and resolutions in data and MC are calibrated using $D^0 \rightarrow \pi^0 \pi^0$ and $B^+ \rightarrow \overline{D}^0 (\rightarrow K^+ \pi^- \pi^0) \pi^+$ decays. The difference is caused by imperfect simulation of the π^0 energy resolution, while the effect of the opening angle distributions can be neglected. The invariant mass distribution for the D^0 is fitted with an empirical function for data and MC, and the observed discrepancies in the peak position and width are converted to the differences in the peak position and resolution for ΔE in the signal PDF. We require the D^0 decay products to lie in the same momentum range as the π^0 s from $B^0 \rightarrow \pi^0 \pi^0$. To obtain the two-dimensional PDF, $P1(M_{bc}, \Delta E)$, for the continuum background, we multiply a linear function for ΔE with the ARGUS function [19] for M_{bc} . The M_{bc} - ΔE PDF for the off-time QED background is modeled as a smoothed two-dimensional histogram using the off-time candidates in the latter data set.

The $P2(\cos \theta_1, \cos \theta_2)$ and $P3(E_{\text{miss}})$ PDFs are described by two-dimensional and one-dimensional smooth histograms, respectively. These PDFs are obtained using the on-time and off-time candidates with trigger timing information. Note that the same on-time PDFs are used for signals, the $\rho^+ \pi^0$ background and the continuum. In other words, these three components are distinguished based on the M_{bc} - ΔE distribution, while the off-time component is identified using all 5 variables. In the fit, the shapes of the signal, off-time and $B^+ \rightarrow \rho^+ \pi^0$ PDFs are fixed and all other fit parameters are allowed to float. We check the modeling of the off-time QED background by comparing the results of the five-dimensional fit to the data with timing information to the fit result using only the M_{bc} - ΔE PDFs after removing the off-time candidates. With 3200 events, the obtained off-time yield from the 5-d fit is 79 ± 14 , consistent with 61 off-time candidates. Moreover, the obtained yields for signals, the $B^+ \rightarrow \rho^+ \pi^0$ background and the continuum are also consistent between the two fits.

We perform a 5-d fit to all the data assuming the same off-time QED distributions for the former and latter data sets. Figure 2 shows the fit projections. The obtained signal yield is $74.4^{+21.4}_{-19.7}$ with a statistical significance (\mathcal{S}) of 5.5σ , where \mathcal{S} is defined as $\mathcal{S} = \sqrt{-2 \ln(\mathcal{L}_0 / \mathcal{L}_{N_s})}$, and \mathcal{L}_0 and \mathcal{L}_{N_s} denote the maximum likelihoods of the fits without and with the signal component, respectively. We vary each calibration constant for the signal PDF by $\pm 1\sigma$ and obtain systematic errors from the change in the signal yield. Adding these errors in quadrature, the systematic error from signal PDF is $^{+3.0\%}_{-3.1\%}$.

In order to obtain the branching fraction, we divide the signal yield by the reconstruction

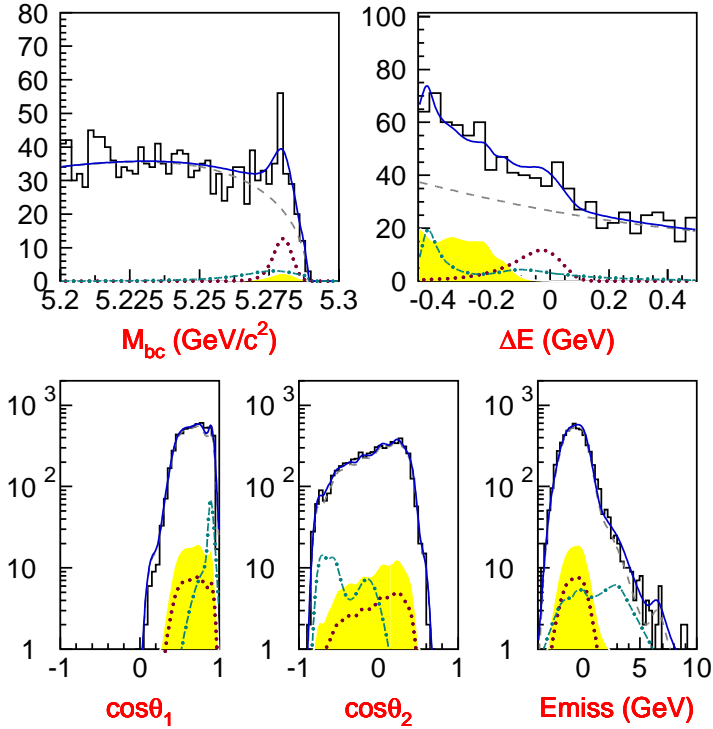


FIG. 2: Result of the fit described in the text. (Top-left) M_{bc} projection for events that satisfy $-0.18 \text{ GeV} < \Delta E < 0.06 \text{ GeV}$; (top-right) ΔE projection for events that satisfy $5.27 \text{ GeV}/c^2 < M_{bc} < 5.29 \text{ GeV}/c^2$. The bottom plots from left to right are $\cos \theta_1$, $\cos \theta_2$ and E_{miss} projections without any M_{bc} and ΔE selection. The solid lines indicate the sum of all components, and the dotted, dashed, dot-dashed lines and hatched part represent the contributions from signal, continuum, off-time and $B^+ \rightarrow \rho^+ \pi^0$ events, respectively.

efficiency, measured from MC to be 12.8%, and by the number of $B\bar{B}$ pairs. We consider systematic errors in the reconstruction efficiency due to possible differences between data and MC. We vary the yields of $\rho^\pm \pi^0$ and off-time events by $\pm 1\sigma$ and obtain the systematic error $^{+4.5\%}_{-4.7\%}$ and $^{+3.1\%}_{-2.3\%}$, respectively. We assign a total error of 8% due to π^0 reconstruction efficiency, measured by comparing the ratio of the yields of the $\overline{D}^0 \rightarrow K^+ \pi^-$ and $\overline{D}^0 \rightarrow K^+ \pi^- \pi^0$ decays. The experimental errors on the branching fractions for these decays [18] are included in this value. We check the effect of the continuum suppression using a control sample of $B^+ \rightarrow \overline{D}^0(\rightarrow K^+ \pi^- \pi^0)\pi^+$ decays; the \mathcal{R}_{sig} requirements has a similar efficiency for the MC control sample and for signal MC. Comparing the \mathcal{R}_s requirement on the control sample in data and MC, a systematic error of 1.5% is assigned. Finally, we assign a systematic error of 1.3% due to the uncertainty in the number of $B\bar{B}$ pairs, $(534.6 \pm 7.0) \times 10^6$, and obtain a branching fraction of

$$\mathcal{B}(B^0 \rightarrow \pi^0 \pi^0) = (1.1 \pm 0.3(\text{stat.}) \pm 0.1(\text{syst.})) \times 10^{-6}.$$

The significance including systematic uncertainties is reduced to 5.4σ .

This new measurement is lower than our previous published result, $(2.3^{+0.4+0.2}_{-0.5-0.3}) \times 10^{-6}$, in which the QED background was considered in the systematic uncertainty. We perform

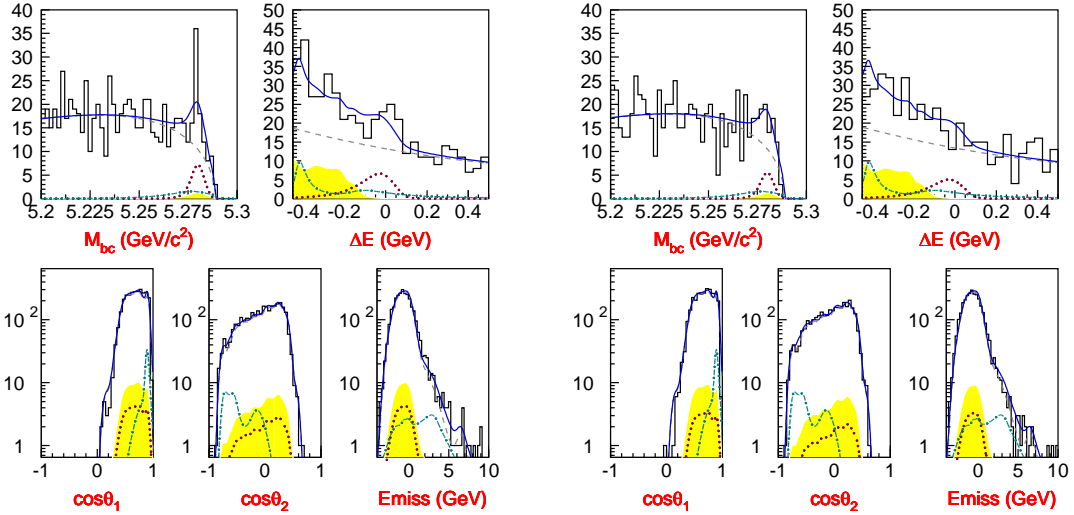


FIG. 3: M_{bc} , ΔE , $\cos \theta_1$, $\cos \theta_2$ and E_{miss} distributions with projections of the fit superimposed. The distributions are shown separately for events tagged as \bar{B}^0 (left) and B^0 (right).

a M_{bc} - ΔE fit to the data used in the previous analysis. Although the current analysis has tighter \mathcal{R}_{sig} requirements to suppress the continuum background, the obtained value of the branching fraction is $(2.0^{+0.5}_{-0.4}) \times 10^{-6}$, consistent with the previous result. We then perform a five-dimensional fit to the same data, the central value of the branching fraction drops to $(1.7 \pm 0.4) \times 10^{-6}$, which is larger than the measurement with 535 million $B\bar{B}$ pairs. We also compare the 2-d and 5-d fit results using the full dataset, the difference of the branching fraction is 0.3×10^{-6} . Therefore, we conclude that the change in the branching fraction is due to a statistical fluctuation and the inclusion of the off-time QED background in the fit, where the former has a larger impact.

The result for \mathcal{A}_{CP} is $0.44^{+0.73+0.04}_{-0.62-0.06}$. Systematic errors are estimated by varying the fitting parameters by $\pm 1\sigma$. Including the errors of wrong-tag fraction (w_k) and the time-integrated mixing parameter (χ_d), the total systematic error is $^{+9.6}_{-17.7}\%$. To illustrate this asymmetry, we show the results separately for B^0 and \bar{B}^0 tags in Fig. 3.

In conclusion, we have improved the measurements of $B^0 \rightarrow \pi^0\pi^0$ in a data sample of 535 million $B\bar{B}$ pairs. We obtain $74.4^{+21.4}_{-19.7}$ signal events with a significance of 5.4 standard deviations (σ) including systematic uncertainties. The branching fraction is measured to be $(1.1 \pm 0.3(\text{stat.}) \pm 0.1(\text{syst.})) \times 10^{-6}$. The branching fraction is different from our previous result due to the larger data sample that is used and the treatment of the off-time QED background. We also report the direct CP asymmetry to be $0.44^{+0.73+0.04}_{-0.62-0.06}$, which is consistent with our previous result [9]. The branching fraction for $B^0 \rightarrow \pi^0\pi^0$, together with the measurements of its direct CP violating asymmetry \mathcal{A}_{CP} , will allow a model-independent extraction of the CKM angle ϕ_2 from measurements of the $B \rightarrow \pi\pi$ system in the near future.

We thank the KEKB group for the excellent operation of the accelerator, the KEK cryogenics group for the efficient operation of the solenoid, and the KEK computer group and the National Institute of Informatics for valuable computing and Super-SINET network support. We acknowledge support from the Ministry of Education, Culture, Sports, Science, and Technology of Japan and the Japan Society for the Promotion of Science; the Australian

Research Council and the Australian Department of Education, Science and Training; the National Science Foundation of China and the Knowledge Innovation Program of the Chinese Academy of Sciences under contract No. 10575109 and IHEP-U-503; the Department of Science and Technology of India; the BK21 program of the Ministry of Education of Korea, and the CHEP SRC program and Basic Research program (grant No. R01-2005-000-10089-0) of the Korea Science and Engineering Foundation; the Polish State Committee for Scientific Research under contract No. 2P03B 01324; the Ministry of Science and Technology of the Russian Federation; the Slovenian Research Agency; the Swiss National Science Foundation; the National Science Council and the Ministry of Education of Taiwan; and the U.S. Department of Energy.

- [1] K. Abe *et al.* (Belle Collaboration), Phys. Rev. D **71**, 072003 (2005).
- [2] B. Aubert *et al.* (BaBar Collaboration), Phys. Rev. Lett. **94**, 161803 (2005).
- [3] M. Kobayashi and T. Maskawa, Prog. Theor. Phys. **49**, 652 (1973).
- [4] K. Abe *et al.* (Belle Collaboration), hep-ex/0608035.
- [5] B. Aubert *et al.* (BaBar Collaboration), hep-ex/0607106.
- [6] M. Gronau and D. London, Phys. Rev. Lett. **65**, 3381 (1990); M. Gronau, D. London, N. Sinha and R. Sinha, Phys. Lett. B **514**, 315 (2001).
- [7] M. Beneke and M. Neubert, Nucl. Phys. B **675**, 333 (2003); Y.-Y. Keum and A.I. Sanda, Phys. Rev. D **67**, 054009 (2003).
- [8] W.S. Hou and K.C. Yang, Phys. Rev. Lett. **84**, 4806 (2000); C.K. Chua, W.S. Hou and K.C. Yang, Mod. Phys. Lett. A **18**, 1763 (2003); A.J. Buras *et al.*, Phys. Rev. Lett. **92**, 101804 (2004).
- [9] Y. Chao, P. Chang *et al.* (Belle Collaboration), Phys. Rev. Lett. **94**, 181803 (2005).
- [10] S. Kurokawa and E. Kikutani, Nucl. Instr. and. Meth. A **499**, 1 (2003), and other papers included in this volume.
- [11] A. Abashian *et al.* (Belle Collaboration), Nucl. Inst. and Meth. A **479**, 117 (2002).
- [12] Z. Natkaniec *et al.* (Belle SVD2 Group), Nucl. Instr. and Meth. A **560**, 1 (2006).
- [13] R. Brun *et al.*, GEANT 3.21, CERN Report No. DD/EE/84-1 (1987).
- [14] The Fox-Wolfram moments were introduced in G. C. Fox and S. Wolfram, Phys. Rev. Lett. **41** 1581 (1978). The modified moments used in this paper are described in Belle Collaboration, S. H. Lee *et al.*, Phys. Rev. Lett. **91**, 261801 (2003).
- [15] R.A. Fisher, Annals of Eugenics **7**, 179 (1936).
- [16] H. Kakuno *et al.*, Nucl. Instr. and Meth. A **533**, 516 (2004).
- [17] S. Villa *et al.* (Belle Collaboration), Phys. Rev. D **73**, 051107(R) (2005).
- [18] Particle Data Group, S. Eidelman *et al.*, Phys. Lett. B **592**, 1 (2004).
- [19] H. Albrecht *et al.* (ARGUS Collaboration), Phys. Lett. B **241**, 278 (1990).